

Constant wWind regimes during the Last Glacial Maximum and early

Formatted: Font: Times New Roman

Holocene: evidence from Little Llangothlin Lagoon, New England Tableland, eastern Australia

James Shulmeister*

School of Geography, Planning and Environmental Management, University of Queensland, St Lucia 4072 Queensland, Australia

* Corresponding author: Ph +61 7 334 61644. Email: james.shulmeister@uq.edu.au

Justine Kemp

Australian Rivers Institute, Griffith University, Nathan 4111 Queensland, Australia

Kathryn E. Fitzsimmons *

Department of Human Evolution, Max Planck Institute for Evolutionary Anthropology,
Deutscher Platz 6, D-04103 Leipzig, Germany

Allen Gontz#

School for the Environment, University of Massachusetts-Boston, Boston MA 02125, USA
#Current Address: Department of Geological Sciences, San Diego State University, San Diego, CA 92182, USA

Formatted: Font: Times New Roman

Abstract

21 Here we present the results of a multi-proxy investigation, integrating geomorphology, ground
22 penetrating radar and luminescence dating, of a high elevation lunette and beach berm in
23 northern New South Wales, eastern Australia. The lunette occurs on the eastern shore of Little
24 Llangothlin Lagoon and provides evidence for a lake high stand combined with persistent
25 westerly winds at the Last Glacial Maximum (LGM - centering on 21.5 ka) and during the early
26 Holocene (c. 9 and 6 ka). The reconstructed atmospheric circulation is similar to the present-day
27 conditions and we infer no significant changes in circulation at those times, as compared to the
28 present day. Our results suggest that the Southern Hemisphere westerlies were minimally
29 displaced in this sector of Australasia during the latter part of the last ice age. Our observations

30 also support evidence for a more positive water balance at the LGM and early Holocene in this
31 part of the Australian sub-tropics.

32

33 **Keywords**

34 Westerlies, last glacial maximum (LGM), lunette, aeolian, lake levels, palaeolimnology,
35 palaeohydrology, ground penetrating radar (GPR), optically stimulated luminescence (OSL)

36

37 **1 Introduction**

38

39 The temperate latitude westerly wind system influences the southern half of the Australian
40 continent, and influences dictates not only this region's climate but also the formation and
41 response of its landscape systems. It plays an important role in the delivery of winter rainfall to
42 the southern half of Australia. Understanding the history of the westerlies in the Australasian
43 region is therefore important for understanding the climate and environmental history of eastern
44 Australia (Shulmeister et al., 2004; Fletcher and Moreno, 2012; Lorrey et al., 2012). In addition,
45 changes in the southern hemisphere westerlies are inferred to modulate global atmospheric
46 carbon dioxide concentrations and potentially trigger global climate changes (e.g. Denton et al.,
47 2010).

48

49 Here we investigate past wind regime changes in eastern Australia as reflected in the shoreline
50 marginal landforms of the Little Llangothlin Lagoon (LLL). LLL is a presently shallow lake
51 which sits at 30 °S (30° 5' 9"S, 151° 46' 53"E) in northern New South Wales. It lies close to the
52 present day northern boundary of the winter westerlies, therefore providing an excellent
53 opportunity to investigate long-term changes in prevailing wind direction and intensity. The
54 lagoon has a lunette (transverse shoreline dune) on its eastern shoreline and a possible beach
55 berm on its south-eastern margin. These landforms reflect aeolian and wave-driven transport and
56 deposition of sediments, and consequently provide indicators for the orientation of prevailing
57 wind directions and intensity at the time of sediment deposition (Bowler, 1968; Bowler, 1973,
58 1983). In this study we undertook luminescence dating, combined with geomorphic and

Formatted: Font: Times New Roman

Formatted: Font: Times New Roman

59 stratigraphic investigations₂ to reconstruct past periods of westerly, and possible north-westerly,
60 prevailing wind flow in this region.

61

62 The endorheic LLL basin was formed in gently undulating tableland comprising Tertiary basalt
63 flows at approximately 1300 m above mean sea level (AMSL). The western shoreline of LLL is
64 dominated by a low ridge of basalt, which rises 30 m above the lake ([see Fig 4](#)[Figure 1](#)). On the
65 eastern side of the basin, the lake is bound by a low hill of granite that forms part of the New
66 England Batholith (Shaw and Flood, 1981). The Lagoon covers an area of 1.2 km² and has a
67 catchment of 3.2 km². LLL is a shallow, roughly circular permanent lake with a maximum depth
68 of 2 m that shallows during droughts, which in this part of Australia are often associated with El
69 Nino years. As far as we can determine, the lake has never dried out fully in post-European
70 settlement times (Woodward et al., 2014b). Another, smaller, lake (Billy Bung Lagoon) lies c.
71 500 m to the southwest of LLL and is separated from the main lake by the low basalt ridge.

72

73

74 The origin of the New England 'lagoons' is cryptic. Conraeds (1989) showed that they were
75 associated with former drainage lines that were occupied by basalt flows. He suggested that
76 uneven infilling of former valleys by basalt during the Tertiary produced shallow depressions
77 where the shallow lakes and swamps, locally called 'lagoons', formed. Similar lakes have been
78 described elsewhere along the tablelands of the Great Dividing Range and Ollier (1979)
79 suggested a tectonic origin for these features, proposing that uplift of the Eastern Highlands
80 caused back tilting on many streams. Other authors such as Bell et al. (2008) have suggested a
81 deflationary origin, where intense weathering occurred as a result of wetting and drying of the
82 basalt. The mechanisms are not incompatible and deflation may have enhanced and maintained
83 the basins₃ which were created by back-tilting.

84

85 Many of these upland lakes have lunettes on their eastern margins (*sensu* Bowler 1976). These
86 are transverse crescentic ridges dominated by wave action and shoreline drift, with coarse
87 textured wave-built ridges on downwind margins (Bowler, 1986). Their regular outline reflects
88 the influence of strong wave action, while the aeolian deflation of sands from the beach forms

89 foreshore dunes with an orientation equivalent toconsistent with the winter wind resultant vector
90 (Bowler, 1971). The proportion of clay and silt in lunettes increases during periods of shoreline
91 regression, and is derived from efflorescence and pelletisation of saline lacustrine sediments on
92 the drying lake floor. Salt concentrations in upland lakes tends to be weakerlow owing to
93 groundwater seepage, restricting the preparation of pelletal clays for deflation and producing
94 dominantly sandy lunettes.

Formatted: Font: Times New Roman

Formatted: Font: Times New Roman

95
96 The catchment is fed by summer rainfall (mean annual rainfall = 880 mm) and has a theoretical
97 net annual moisture balance deficit of c. 400 mm (Woodward et al., 2014a). The regional
98 vegetation is dominated by montane open eucalypt woodland, while the lagoon itself contains
99 extensive beds of tall spike rush *Eleocharis sphacelata* and the water plant *Potamogeton*
100 *tricarinatus* in the deeper parts of the basin. Other swamp plants, including *Carex*
101 *glaudichaudiana*, are dominant in the surrounding wet margins of the lagoon.

Formatted: Font: Times New Roman

102
103 The lagoon has been intensively investigated from a palaeoecological and environmental
104 viewpoint because it is a major bird reserve as well as a Ramsar wetland. Furthermore, the site
105 has been identified as a location of exceptional soil erosion since European settlement (Gale et
106 al., 1995; Gale and Haworth, 2005), although this has recently been challenged (Woodward et
107 al., 2011). The site has more recently become a focus for work due to inferred changes to basin
108 hydrology in response to tree clearance during European settlement of the New England
109 Tablelands (Woodward et al., 2014a). There has also been some investigation of the
110 archaeological history of the lagoon suggesting that landscapes such as these provided relatively
111 rich resources for Aboriginal people, and that New England lagoons became the foci for
112 ceremonial activities, although the degree to which hydrological conditions influenced human
113 activity remains poorly understood since chronological control for the pre-European period has
114 so far been lacking (Beck et al., 2015).

115
116 This paper examines the geomorphic context of shoreline features on the western and southern
117 margins of the lagoon and focuses on the history of lake-margin sediment deposition to
118 reconstruct the climatic circulation from the last glacial maximum (LGM) into the Holocene.

119
120
121
122
123

2 Materials and Methods

2.1 Field investigations

124 Transects across an apparent beach berm and the lunette were surveyed using a MALA ProEx
125 ground penetrating radar (GPR) system with a 500 MHz antenna and integrated high-resolution
126 GPS. The GPR data were collected in transects forming a rough grid parallel and perpendicular
127 to the trend of hypothesised beach and lunette landforms. The GPR was hand-dragged at a
128 speed of ~ 4 kph and fired using time firing at a rate of 10 Hz resulting in an average along-track
129 resolution of 0.11 m and 0.07 m vertical resolution, based on a center frequency of 500 MHz.
130 After acquisition, radar data were processed using GPR Slice software (DC drift; user-defined
131 signal gain; bandpass lo=350 MHz, hi=650 MHz; background removal). Profiles were
132 topographically corrected using elevation data from the GPS system and spot-checked using
133 known elevations. While absolute topography was not reliable, relative elevation was
134 consistently reproducible. Individual profiles were converted to depth-distance using the
135 published radar velocity for wet sands of 0.07 m/ns in the beach ridges and dry sands 0.12 m/ns
136 in the lunette (Neal, 2004). Depth-distance profiles were used to evaluate sediment thickness and
137 observe true geometry of radar reflectors.

Formatted: Font: Times New Roman

138
139
140
141
142
143
144
145
146
147
148

The sub-surface sediments were logged using a hand auger to a depth of between 0.6 m and 1.2 m, depending on sub-surface conditions. Sub-samples were collected for grain size analyses. In addition, gravels from the sand and gravel barrier were treated with HCl for 12 hours in order to identify weathering products such as manganese–iron pisoliths. Four samples were collected for optically stimulated luminescence (OSL) dating using steel tubes, wrapped in black plastic, and transported to the Max Planck Institute for Evolutionary Anthropology in Leipzig for analysis.

Formatted: Font: Times New Roman, 12 pt

Formatted: Font: Times New Roman

149 Anthropology in Leipzig. The OSL samples were prepared under subdued red light using
150 published methods (Fitzsimmons et al., 2014). This involved sieving, applying treatments-HCl
151 acid and hydrogen peroxide digestion to remove carbonates and organic matter respectively, and
152 isolating pure, 180-212 μm quartz grains. The outer $\sim 10 \mu\text{m}$ alpha-irradiated rind of each grain
153 was removed by etching in hydrofluoric acid, and the sample was then subjected to a final sieve
154 to remove finer fragments which had broken off during etching. The quartz grains were then
155 prepared as small aliquots (18 discs; 1 mm diameter) for preheat testing and as single grains (600
156 grains; 6 single grain discs) for equivalent dose (D_e) measurement.

157

158 D_e measurements were undertaken using an automated Risø TL-DA-15 equipped with blue light-
159 emitting diodes (for preheat and initial dose estimate testing), and a TL-DA-20 reader with a
160 single grain attachment containing a green laser emitting at 532 nm, for light stimulation of
161 single aliquots and single grains respectively (Botter-Jensen et al., 2000). Irradiation was
162 provided by calibrated $^{90}\text{Sr}/^{90}\text{Y}$ beta sources. Equivalent doses were determined on single grains
163 using the single aliquot regenerative dose (SAR) protocol of Murray and Wintle (2000; 2003).
164 Preheat temperatures of 260°C were chosen based on the results of the preheat plateau tests
165 (Figure S24) for the natural and regenerative doses, with a preheat temperature of 220°C for the
166 test doses (0.94 Gy).

167

168 Individual grains were analysed for their suitability for OSL dating based on the selection criteria
169 of Jacobs and Roberts (2007). The single grain dose distributions of all samples are >40%
170 overdispersed with complex dose populations (Table S1), and therefore the Finite Mixture Model
171 (FMM) was used to identify dose populations (Galbraith and Green, 1990). The OSL dating
172 results are summarised in Table 1. Equivalent dose distributions for the four samples are shown
173 as radial plots, with the FMM-derived dose populations highlighted, in Figure 3-S34.

174

175 2.3 OSL dating - Dose rate calculations

176 Uranium, thorium and potassium (^{40}K) activities were measured in the “Felsenkeller” laboratory
177 at VKTA Rossendorf in Dresden, Germany, using low-level gamma-ray spectrometry. Dose
178 rates were calculated using the conversion factors of Stokes et al. (2003) with β -attenuation

Formatted: Font: Times New Roman

Formatted: Font: Times New Roman

Formatted: Font: Times New Roman, Not Highlight

Formatted: Font: Times New Roman

179 factors taken from Mejdahl (1979). Beta counting was based on 1 g homogenized subsamples
180 and used for the beta component of the dose rate. Measured water contents ranged from 5-10%
181 and these values were used for all samples. Cosmic dose rates were calculated from Prescott and
182 Hutton (1994).

183

184 **3 Results**

185

186 *3.1 Geomorphology*

187 There are no dune or beach deposits on the western side of the lake (Figure 1). The main
188 geomorphic feature on the eastern side of the lake is ~~a the lunette small dune system~~ and the low
189 basalt ridge. The ~~dunefield lunette~~ comprises a north-south oriented ridge less than 2 m high
190 adjacent to the lake, a swale behind that is occupied by a small stream and a small sand flat area
191 that extends up to 50 m east of the lake shore.

192

193 The lunette on the eastern shore is composed of poorly sorted medium sand grading upwards into
194 fine sand with accessory silt contents of 3-15%. Particle size results and other stratigraphic
195 information are plotted on Figure 1 and particle size analysis curves are provided as
196 Supplementary Figure 1. GPR transects are shown in Figures 2a and 2b.

197

198 On the SE margin of LLL, there is a partly infilled outlet, immediately to the west of which is a
199 c. 100 m long, 50 m wide low (< 1m) berm. The berm is poorly to well sorted, medium and
200 coarse quartz rich sand with iron-manganese, pisolithic gravel and a silt content of 1-14%.

201

202 *3.2 GPR results*

203

204 The GPR proved effective at mapping stratigraphic architecture and subsurface character to a
205 depth shallower than 4 m in the berm (Figures 2a and 2b). GPR data suggest the presence of
206 several distinct units related to changes in lake level and the development of spit/barrier and
207 berm formations (Shan et al., 2015; Thompson et al., 2011). The berm showed strong internal
208 stratification ~~on-and~~ features perpendicular lines with strong sigmoidal clinoforms indicating

Formatted: Font: Times New Roman

Formatted: Font: Times New Roman

209 beach progradation to the west (Thompson et al., 2011) as well as low-angle sub-parallel
210 reflectors dipping to the east suggesting basin infill via over wash processes. This package is
211 underlain by a convex-up package of reflections that are sub-parallel with dips to the east and
212 west. Comparison of this feature with those identified by Shan and others (2015)
213 suggest the complex is underlain by a spit complex. Additional information on the character of
214 the lower units associated with the interpreted spit are unavailable due to the existing GPR data
215 coverage.

216
217 The internal stratigraphy of the fine-grained lunette was difficult to assess with the GPR.
218 Evidence of extensive modern bioturbation by rabbits was observed during the radar acquisition.
219 The shallow penetration did however show weak internal characteristics commonly associated
220 with lunette formation (Thomas and Burrough, in press). These included eastward dipping high
221 angle reflectors that are truncated on the western facing slope, coupled with areas of parallel to
222 sub-parallel reflections that change to steeply dipping reflections. All reflectors are laterally
223 discontinuous and show evidence of disturbance at all depths observed, rendering the GPR data
224 ineffective at determining genetic processes or detailed landform characteristics.

225
226 *3.3 OSL results*
227
228 The OSL age data are summarised in Table 1, and shown with respect to stratigraphy and
229 catchment geomorphology in Fig 1. The three samples collected from three different locations
230 along the lunette suggest that the entire landform was formed active during the LGM, between c.
231 24-19 ka. Our samples do not extend to the base of aeolian sedimentation and it is likely that the
232 lunette was formed earlier than the LGM. The secondary age populations identified by FMM are
233 all younger than the LGM main phase of deposition (Figure 3; Table S2-S32) and suggest phases
234 of partial reactivation or pedogenic infiltration of material into the lunette. The younger age
235 populations from sites LL3 and LL4 in the central part of the lunette are comparable and strongly
236 suggest contemporaneous post-depositional infiltration of younger material or partial reactivation
237 of the lunette in the early Holocene (c. 9-8 ka; Table S2). Sample L-EVA 1230 (LL3) exhibits a
238 third peak centred on 11.8 Gy (9.1 ka). The second major age population from the LL2 site in

Formatted: Font: Times New Roman, Not Highlight

Formatted: Font: Times New Roman

239 the southern part of the lunette dates to the mid-Holocene (5.6 ± 0.5 ka; Table S2) and suggests
240 spatial and temporal variability in the Holocene post-depositional pedogenesis (or reactivation)
241 of the lunette.

242
243 The overdispersion on individual D_e results from the berm was too high (79.9%; Table S1) to
244 reliably define a depositional age, although the largest age population yields a mid-Holocene age
245 (5.1 ± 0.5 ka; Table 1) comparable with the reactivation of the southern part of the lunette at
246 LL2. The minor dose populations yield ages of 11.1 ± 1.6 ka, 2.3 ± 0.3 ka and 1.2 ± 0.1 ka
247 (Table S2).

248

249 **4 Discussion**

250

251 There are two separate but related sets of geomorphic features recorded along the eastern and
252 south-eastern margin of LLL. These are the sand and gravel berm which is a lake beach/spit
253 feature and the lunette which is an Aeolian feature but tied to the shoreline. Both are supplied
254 with sediment by wind wave processes in the lake but the former is a sub-aqueous feature, while
255 the lunette is an Aeolian structure.

256

257 *4.1 A possible spit/barrier berm on the SE corner of the lagoon*

258

259 The most cryptic landform in the basin is the barrier sand and gravel berm feature on the SE
260 margins of LLL. The feature was identified by Gale et al. (2005), who interpreted it as part of a
261 relict older lunette feature. From visual observations alone, this is a reasonable interpretation
262 because the low berm does look like the erosional shadow of an older ridge. Our sedimentologic
263 and GPR structural investigations, however, discount this interpretation. Based on both GPR and
264 field observations from pits, the feature is clearly a beach berm, with numerous small wash-over
265 structures (see Fig. 2a).

266

267 The berm barrier feature is composed of pea-sized gravels within a finer sandy matrix. We
268 assume the sandy matrix to be post-depositional because it is incompatible with the sedimentary

← **Formatted:** Indent: Left: 0 cm

Formatted: Font: Times New Roman, Not Bold

Formatted: Font: Times New Roman

Formatted: Font: Times New Roman, Not Bold

Formatted: Font: Times New Roman

269 structures and post-depositional infilling of openwork deposits is common. In addition, the
270 contrast between locally sourced detrital basalts and reworked quartz-rich sand and silt is
271 striking. The matrix may have accumulated either through aeolian accession, or through
272 filtration of sands through the barrier during high lake stands when the berm would have acted as
273 a permeable filter for the lake. Given the mostly coarse nature of the matrix (medium to coarse
274 sand), we prefer the two-stage filtration hypothesis.

275

276 The pea-sized gravels are detrital. We suggest that the most likely origin for this feature is as a
277 spit that developed from the basalt ridge on the SW edge of the lake, and that the basalt gravels
278 were moved along the shoreline by longshore drift. The barrier ultimately cut off an area to the
279 SW of the present lake that was part of a larger, ancestral lake feature, for which we have no age
280 constraint due to the lack of associated sedimentary deposits. The barrier post-dates the LGM as
281 we have been provided with a radiocarbon result (R. Haworth pers comm 2016) from a depth of
282 1.5 m close to our LL1 sample (Beta-110588 16,200 ± 70 yr BP: median 19500 cal yr BP:
283 calibration from Stuiver and Reimer, 1993 (Calib 7.1) with a Southern Hemisphere correction
284 (SHCal13) from Hogg et al., 2013) that provides a maximum age for the barrier. The
285 luminescence sample based on the finer matrix material at 0.5 m depth yielded a highly dispersed
286 dose distribution with four age populations, which is not unexpected given our hypothesis that
287 the matrix is post-depositional. The grains may represent the accretion of fines to the barrier
288 during high stands in the lake in the early (c. 11 ka), mid (c. 5.6 ka) and late Holocene (c. 2.3 ka,
289 1.2 ka).

290

291 *4.2 Aeolian history of LLL from the lunette*

292

293 Based on the morphology, sedimentary composition and internal structure, the feature along the
294 eastern shoreline of LLL is clearly a composite beach and aeolian landform. The quartz-rich
295 sands were most likely derived from the granites on the eastern side of the catchment, which
296 deposited into the lake and were subsequently reworked onto the shoreline. Curiously, even
297 though half the basin is comprised of basalt, yet there is little evidence for basalt-derived
298 sediments in the lunette system. By contrast, the fine sediments in the depocentre of the lake

Formatted: Font: Times New Roman

Formatted: Font: Times New Roman

299 basin are primarily derived from basalt (e.g. Woodward et al., 2011). This implies that there is an
300 effective sorting mechanism within the basin, whereby, ~~the basalt preferentially weathers to~~
301 ~~mud while the granite generates sand. Current sorting by currents would move transport~~ the
302 ~~fines to the depocentre while the sands would be moved transported~~ towards the lake margins.
303 The ~~obvious most parsimonious~~ candidate for this ~~latter~~ process is wind-blown waves.

304
305 Present day wind roses for LLL (BOM, 2014) demonstrate that there are two primary wind
306 directions (Figure 4), one from the east and the other from the west to north-west. These
307 prevailing winds have strong seasonal components. Winter winds (August) are dominated by
308 westerlies and provide the strongest and most persistent flows (8% calm) consistent with
309 eastward transport and deposition of sediments onto a lunette situated on the eastern shoreline of
310 LLL. Summer winds (February) are dominated by easterlies associated with onshore circulation
311 on the northern limb of the sub-tropical high pressure cell in summer (Fig. 4). These easterly
312 winds are on average weaker (20% calm) but do include short periods of relatively high intensity
313 winds, which might be expected to result in sediment transport to, and deposition onto, the
314 western side of the lake. It is curious therefore that all depositional landforms marginal to LLL
315 are located on the east and south-east sides of the lake, with no deposition on the western
316 shoreline. ~~Examination of the wind roses indicates that sand transporting winds (above ~22 kmh;~~
317 ~~Fryberger, 1979) was more than twice as frequent (~14% versus ~5%) in –August than in~~
318 ~~February, and that the highest wind speeds occurred more frequently in August. This indicates~~
319 ~~confirms~~ that the most effective net sand-transporting wind, associated with lunette and berm
320 formation, was from the west/north-west. The transport is most likely to have been primarily
321 sub-aqueous, since the relatively poor sorting in the foredune indicates only ~~intermittent-a short-~~
322 ~~distance aeolian transport pathway, at least of the coarsest component.~~

323
324 One obvious question is why the westerlies are so strongly recorded in the LLL lunette, and not
325 the easterlies. This partly reflects the greater frequency of high wind speeds from the west, but
326 ~~on its own it is unlikely to explain the entire phenomenon~~
327 ~~In addition to the stronger drift~~
328 ~~potential there may also be a biological effect also.~~ The most parsimonious answer integrates the
sedimentary information with seasonal variations in the biological system. The rush beds

329 occurring in the shallower parts of the lake are most fully developed during the summer. Unlike
330 much of Australia, winters are severe on the New England Tablelands due to the relatively high
331 elevations, and seasonal die-back of the jointed wire-tall spike rush is also observed today. New
332 growth emerges in spring and dies off in autumn in cooler, high altitude sites (Rajapaskse et al.,
333 2006). Consequently, the summer peak in vegetation cover disrupts the wind fetch over the lake
334 precisely at the same time as the easterly winds penetrate the tablelands, thereby further reducing
335 the ability for waves to set up during the warmer months.

336

337 The luminescence ages from the lunette are coherent. ~~+~~ All ~~three~~ samples are dominated by
338 grains that are LGM in age. The samples all overlap at 2σ and produce a weighted mean age of
339 20.4 ± 0.8 ka ~~mean age of 21.5 ka~~, indicating that the main phase of dune activity at LLL occurred
340 during the late LGM. Our interpretation that the dominant sediment transport mechanism was
341 subaqueous therefore implies that the LGM oversaw permanent, and probably full, lake
342 conditions at LLL. Evidence from our unpublished pollen records and sedimentary archives
343 from the depocentre of the lake support the concept support our hypothesis offer a full lake
344 during the late LGM (c. 19 ka). Specifically, the lake sediments from this time interval are an
345 unoxidised grey clay, which contains numerous sponge spicules. In addition, pollen records from
346 these latitudes suggest the survival of rainforest at lower elevations to the east through the LGM
347 (e.g. Moss et al., 2013), indicating persistence of moisture availability. Our argument for the
348 persistence, and perhaps intensification, of winter westerlies throughout the LGM at LLL is also
349 confirmed by observations made at North Stradbroke Island some 300 km to the north-northeast
350 of our site (Petherick et al., 2009; McGowan et al. 2009). North Stradbroke Island lies at the very
351 northern edge of the westerlies zone, and the accession of fine aeolian material into a dune lake
352 there indicates that the winter westerlies were operative at the LGM in South East Queensland at
353 27.20°S (Petherick et al., 2009; McGowan et al. 2009), just as the westerlies operate today in this
354 region.

355

356 A secondary peak in grain ages is observed ~~from-in~~ all three lunette samples. This peak is less
357 well defined but in all three cases relates to the early to mid-Holocene between 9 and 6 ka. Work
358 from the lake (Woodward et al., 2011) has already demonstrated that the early Holocene was the

Formatted: Font: Times New Roman

359 last phase, before the modern anthropogenically modified lake, with lake full conditions as
360 represented by extensive *Eleocharis* beds. Wind waves would We have been effective on the
361 lake and we infer partial reactivation of the lunette at thisthis times.

362
363 We note a third grain age peak in one lunette sample (EVA1230) at c. 3 ka. This is both the
364 weakest individual age peak and not replicated at any other site. It is possible that this represents
365 a dune re-activation event, bioturbation, or even Aaboriginal usage of the site which has been
366 proposed to have intensified during the late Holocene (post 4300 yr; Beck et al., 2015). At this
367 stage this event, if real, is still poorly controlled chronologically and we do not interpret it
368 further.

369
370 Overall, our evidence demonstrates that at the LGM, winter westerly winds were strong enough
371 to form the eastern shoreline lunette in a single phase, with possible later reactivation during the
372 early Holocene. Critically, foredune activation depends as much on high water levels in the lake
373 allowing the wave delivery of sediment to the eastern beach as it does on sand mobilizing winds
374 (Bowler, 1983). During the Pleistocene, elevations above 800 m in the region were subject to
375 extensive, active development of block deposits, scree, and solifluction lobes, indicating winter
376 cooling of at least 10.5 °C relative to present (Slee and Shulmeister, 2015). Reduced evaporation
377 due to lower temperatures (e.g. Hesse et al., 2003) and transfer of flow from
378 throughflow/baseflow to overland flow due to increased snow cover (Reinfelds et al., 2014) at
379 this time is likely to have been sufficient to cause the change to a positive hydrological balance
380 in the lake.

381
382 For the intervening periods, at least in the Holocene, the evidence (Woodward et al., 2014a)
383 suggests that water levels were lower and/or even that the lake was ephemeral. It is highly
384 unlikely that sand would be transported to the high stand beach during low lake levels. If the
385 entire basin floor fully dried out, pelletised clays might be expected, and yet none are observed.
386 There are two likely reasons for this. Firstly, this high elevation site is unlikely to become very
387 arid even during relatively dry phases when swampy conditions probably persisted on the basin
388 floor. Similarly, it is unlikely that salt formation is significant in this setting and clay

Formatted: Font: Times New Roman
Formatted: Font: Times New Roman

389 pelletisation may not occur. This is similar to observations from Lake George, which also ~~occurs~~
390 lies within a cool temperate climate setting along the Great Dividing Range (Fitzsimmons and
391 Barrows, 2010).

392
393 In summary, these records strongly suggest that for the two intervals recorded (the LGM and
394 early Holocene), the overall circulation conditions at LLL were very similar to the present day.
395 This region presently lies near the northern limit of westerly penetration in winter. ~~Westerlies~~
396 ~~occurred during both the early Holocene and the LGM suggesting that at both time intervals the~~
397 ~~position of the westerly jet lay near 30°S, which is its modern track.~~ For the intervening periods,
398 absence of evidence is not evidence of absence, and if the winter westerly winds lay at this
399 latitude during peak warming in the early Holocene and during the LGM, it seems reasonable to
400 suppose that this track has been persistent over the last 25 ky.

401
402 The track of the Australian winter westerlies during the LGM has been a source of contention for
403 some time, with both poleward and equatorward changes argued for (e.g. Harrison and Dodson,
404 1993; Hesse, 1994; Shulmeister et al., 2004). One possibility is that the westerly lay north of its
405 current track during the LGM and that the timing of the westerlies at LLL shifted seasonally. A
406 northward shift of ~3° (350 km) in the position of the westerly wind belt during MIS 2 was
407 recorded in sediments from marine cores in the Tasman Sea (Hesse, 1994). Analysis of the
408 aeolian component of lake sediments on North Stradbroke Island at 27 °S for the period 25-22 ka
409 indicates dust sources in the SW Murray-Darling Basin, with a secondary component from
410 WNW of the site (Petherick et al. 2009). These findings are consistent with either no change or
411 is lends support to a possible northward shift in the westerlies but are not consistent with the
412 poleward contraction of the westerlies in eastern Australia at the LGM.

413
414 **Conclusions**

415
416 This study indicates that westerly winds ~~construeactivatedted~~ a ~~foredune ridge lunette~~ at LLL
417 during the LGM under the influence of high lake levels. This ridge was reactivated during high
418 lake stands in the early to mid-Holocene. The persistence of westerly winds at this site during the

419 LGM confirms observations from North Stradbroke Island at the northern limits of penetration of
420 the temperate latitude westerlies. This suggests that the overall circulation pattern in this part of
421 eastern Australia, at the modern northern limits of westerly winter flow, remained constant
422 during both the LGM and the early Holocene. Overall, this points to minimal change in
423 circulation patterns over the last 25 ky.

424

425 **Team List**

426 James Shulmeister

427 Justine Kemp

428 Kathryn Fitzsimmons

429 Allen Gontz

430

431 **Copyright Statement**

432
433 Except where explicitly acknowledged the authors hold the copyright of the materials presented.

434

435 **Author Contributions**

436 J Shulmeister lead the project, assisted with field sampling for OSL and grain size and lead the
437 manuscript development. J Kemp assisted in the field with OSL sample acquisition, conducted
438 grain size analysis and participated in manuscript development. K Fitzsimmons oversaw
439 undertook the OSL sample analysis and participated in manuscript development. A Gontz lead
440 the GPR acquisition and processing, assisted with OSL sampling and manuscript development.

441

442 **Acknowledgements**

443 This research was funded by an Australian Research Council Discovery Grant DP110103081,
444 “The last glaciation maximum climate conundrum and environmental responses of the Australian
445 continent to altered climate states”. We thank S. Hesse for assistance with OSL sample
446 preparation. R. Haworth made a radiocarbon age from underneath the sand and gravel berm
447 available to us. C. Woodward, J. Chang, and A. Slee assisted with fieldwork. We thank all the

Formatted: Font: Times New Roman, German (Germany)

Formatted: Font: Times New Roman

Formatted: Font: Times New Roman

Formatted: Font: Times New Roman

448 referees for very helpful input that has improved the paper. We thank NSW Parks and Wildlife
449 Service for access to the site and the local farmers for retrieving our vehicle from the bottomless
450 suck hole!

Formatted: Font: Times New Roman

451 452 References

453 Bell, D.M., Hunter, J.T., and Haworth, R.J.: Montane lakes (lagoons) of the New England
454 tablelands bioregion, Cunninghamia, 10, 475-492, 2008.

455 Beck, W., Haworth, R., and Appleton, J.: Aboriginal resources change through time in New
456 England upland wetlands, south-east Australia, Archaeol Ocean. 50, 47-57, 2015.

Formatted: Font: (Default) Times New Roman

457 Botter-Jensen, L., Bular, E., Duller, G.A.T., and Murray, A.S.: Advances in luminescence
458 instrument systems, Radiat Meas, 32, 523-528, 2000.

459 Bowler, J.M.: Aridity in Australia: age, origins and expression in aeolian landforms and
460 sediments, Earth Sci Rev, 12, 279-310, 1976.

461 Bureau of Meteorology. Summary statistics Guyra Hospital. Climate Data Online. 2014.
462 Available at: http://www.bom.gov.au/climate/averages/tables/cw_056229.shtml. Last accessed.
463 29 February, 2016.

Formatted: Font: (Default) Times New Roman

Formatted: Font: (Default) Times New Roman

464 Coenraads, R.R.: Evaluation of the natural lagoons of the Central Province, NSW—Are they
465 sapphire-producing maars?, Explor Geophys, 20, 347-363, 1989.

466 Denton, G.H., Anderson, R.F., Toggweiler, J.R., Edwards, R.L., Schaefer, J.M., Putnam, A.E.:
467 The last glacial termination. Science, 328 (5986):1652-6. doi: 10.1126/science.1184119, 2010.

468 Fitzsimmons, K.E., and Barrows, T.T.: Holocene hydrologic variability in temperate
469 southeastern Australia: An example from Lake George, New South Wales, The Holocene 20,
470 585-59, 2010.

471 Fitzsimmons, K.E., Stern, N., and Murray-Wallace, C.V.: Depositional history and archaeology
472 of the central Lake Mungo lunette, Willandra Lakes, southeast Australia, J Archaeol Sci 41, 349-
473 364, 2014.

474 Folk, R.L. Petrology of Sedimentary Rocks, Hemphill, Austin, 1974.

Formatted: Font: Times New Roman, 12 pt

Formatted: Font: (Default) Times New Roman

475
476 Fletcher, M.S., and Moreno, P.I.: Have the Southern Westerlies changed in a zonally symmetric
477 manner over the last 14,000 years? A hemisphere-wide take on a controversial problem,
478 Quaternary Int, 253, 32-46, 2012.

479

480 Fryberger, S.G.: Dune forms and wind regime. In: A study of global sand seas. McKee, E.D.
481 (Ed) Gov print office, Washington, USA, 137-160, 1979.

482 Galbraith, R.F., and Green, P.F.: Estimating the component ages in a finite mixture, Nucl Tracks
483 Rad Meas 17, 197-206, 1990.

484 Gale, S.J., Haworth, R.J., and Pisanu, P.C.: The 210 Pb chronology of late Holocene deposition
485 in an eastern Australian lake basin, Quaternary Sci Rev, 14, 395-408, 1995.

486 Gale, S.J., and Haworth, R.J.: Catchment-wide soil loss from pre-agricultural times to the
487 present: transport-and supply-limitation of erosion. Geomorphology, 68, 314-33, 2005.

488 Haworth, R.J., Gale, S.J., Short, S.A., and Heijnis, H.: Land use and lake sedimentation on the
489 New England tablelands of New South Wales, Australia, Aust Geogr, 30, 51-73, 1999.

490 Harrison, S.P., and Dodson, J.R.: Climates of Australia and New Guinea since 18,000 yr B.P. In:
491 Wright Jr., H.E., Kutzbach, J.E., Webb III, T., Ruddiman, W.F., Street-Perrot, F.A., Bartlein, P.J.
492 (Eds.), Global Climates Since the Last Glacial Maximum. University of Minnesota Press,
493 Minneapolis, MN, 265-293, 1993.

494 Hesse, P.P.: The record of continental dust from Australia in Tasman Sea sediments, Quaternary
495 Sci Rev, 13, 257-72, 1994.

496 Hesse, P.P., Humphreys, G.S., Selkirk, P.M., Adamson, D.A., Gore, D.B., Nobes, D.C., Price,
497 D.M., Schwenninger, J-L., Smith, B., Tulau, M., Hemmings, F.: Late Quaternary aeolian dunes
498 on the presently humid Blue Mountains, Eastern Australia, Quat Int, 108, 13-32, 2003.

499 Hogg, A.G., Hua, Q., Blackwell, P.G., Buck, C.E., Guilderson, T.P., Heaton, T.J., Niu, M.,
500 Palmer, J.G., Reimer, P.J., Reimer, R.W., Turney, C.S.M., Zimmerman, S.R.H.,
501 Radiocarbon, 55, DOI: 10.2458/azu_js_rc.55.16783, 2013.

502 Jacobs, Z., and Roberts, R.G.: Advances in optically stimulated luminescence dating of
503 individual grains of quartz from archeological deposits, Evol Anthropol, 16, 210-223, 2007.

504 Lorrey, A.M., Vandergoes, M., Almond, P., Renwick, J., Stephens, T., Bostock, H., Mackintosh,
505 A., Newnham, R., Williams, P.W., Ackerley, D., and Neil, H.: Palaeocirculation across New
506 Zealand during the last glacial maximum at ~21 ka, Quaternary Sci Rev, 36, 189-213, 2012.

507 McGowan, H.A., Petherick, L.M., and Kamber, B.S.: Aeolian sedimentation and climate
508 variability during the late Quaternary in southeast Queensland, Australia, Palaeogeog, Palaeocl,
509 265, 171-81, 2008.

Formatted: Font: (Default) Times New Roman

Formatted: Font: (Default) Times New Roman

510 Mejdahl, V.: Thermoluminescence dating: beta-dose attenuation in quartz grains, Archaeometry
511 21, 61-72, 1979.

512 Moss, P.T., Tibby, J., Petherick, L., McGowan, H. and Barr, C.: Late Quaternary vegetation
513 history of North Stradbroke Island, Queensland, eastern Australia, Quaternary Sci Rev, 74, 257-
514 272, 2013.

515 Murray, A.S., and Wintle, A.G.: Luminescence dating of quartz using an improved single-aliquot
516 regenerative-dose protocol, Radiat Meas, 32, 57-73, 2000.

517 Murray, A.S., and Wintle, A.G.: 2003. The single aliquot regenerative dose protocol: potential
518 for improvements in reliability, Radiat Meas, 37, 377-381, 2003.

519 Neal, A.: Ground penetrating radar and its use in sedimentology: principles, problems and
520 progress, Earth Sci Rev, 66, 261-330, 2004.

521 Ollier, C.D.: Evolutionary Geomorphology of Australia and Papua: New Guinea, T I Brit Geog,
522 4, 516-39, 1979.

523 Petherick, L.M., McGowan, H.A., and Kamber, B.S.: Reconstructing transport pathways for late
524 Quaternary dust from eastern Australia using the composition of trace elements of long traveled
525 dusts, Geomorphology, 105, 67-79, 2009.

526 Prescott, J.R., and Hutton, J.T.: Cosmic ray contributions to dose rates for luminescence and
527 ESR dating: Large depths and long term variations, Radiat Meas, 23, 497-500, 1994.

528 Rajapakse L., Asaeda, T., Williams, D., Roberts, J., and Manatunge, J.: Effects of water depth
529 and litter accumulation on morpho-ecological adaptations of Eleocharis sphacelata, Chem Ecol,
530 22, 47-57, 2006.

531 Reinfelds, I., Swanson, E., Cohen, T., Larsen, J., and Nolan, A.: Hydrospatial assessment of
532 streamflow yields and effects of climate change: Snowy Mountains, Australia, Jour Hydrol, 512,
533 206-220, 2014.

534 Shan, X., Yu, X., Clift, P.D., Tan, C., Jin, L., Li, M, and Li, W.: The ground penetrating radar
535 facies and architecture of a paleo-spit from Huangqihai Lake, North China: implications for
536 genesis and evolution, Sediment Geol, 323, 1-14, 2015.

537 Shaw, S.E., and Flood, R.H.: The New England Batholith, eastern Australia: geochemical
538 variations in time and space, J Geophys Res-Sol Ea, 86, 10530-10544, 1981.

539 Shulmeister, J., Goodwin, I., Renwick, J., Harle, K., Armand, L., McGlone, M.S., Cook, E.,
540 Dodson, J., Hesse, P.P., Mayewski, P., and Curran, M.: The Southern Hemisphere westerlies in
541 the Australasian sector over the last glacial cycle: a synthesis, Quaternary Int, 118, 23-53, 2004.

542 Slee, A., and Shulmeister, J.: The distribution and climatic implications of periglacial landforms
543 in eastern Australia, *J Quaternary Sci*, 30, 848-58, 2015.

544 Stokes, S., Ingram, S., Aitken, M.J., Sirocko, F., Anderson, R., and Leuschner, D.: 2003.
545 Alternative chronologies for Late Quaternary (Last Interglacial–Holocene) deep sea sediments
546 via optical dating of silt-sized quartz, *Quaternary Sci Rev*, 22, 925-941, 2003.

547 [Stuiver, M., and Reimer, P.J., Radiocarbon, 35, 215-230, 1993.](#)

Formatted: Font: (Default) Times New Roman

548 Thomas, D.S.G., and Burrough, S.L.: Luminescence-based chronologies in southern Africa:
549 analysis and interpretation of dune database records across the subcontinent, *Quaternary Int*, 1-
550 16, in press.

551 Thompson, T.A., Lepper, K., Endres, A.L., Johnston, J.W., Baedke, S.J., Argilan, E.P., Booth,
552 R.K., and Wilcox, D.A.: Mid Holocene lake levels and shoreline behaviour during the Nipissing
553 phase of the upper Great Lakes at Alpena, Michigan, USA, *J Great Lake Res*, 37, 567-576, 2011.

554 Woodward, C., Chang, J., Zawadzki, A., Shulmeister, J., Haworth, R., Collecutt, S., and
555 Jacobsen, G.: Evidence against early nineteenth century major European induced environmental
556 impacts by illegal settlers in the New England Tablelands, south eastern Australia, *Quaternary*
557 *Sci Rev*, 30, 3743-3747, 2011.

558 Woodward, C., Shulmeister, J., Bell, D., Haworth, R., Jacobsen, G., and Zawadzki, A.: A
559 Holocene record of climate and hydrological changes from Little Llangothlin Lagoon, south
560 eastern Australia, *The Holocene*, 6:0959683614551218, 2014a.

561 Woodward, C., Shulmeister, J., Larsen, J., Jacobsen, G.E., and Zawadzki, A.: The hydrological
562 legacy of deforestation on global wetlands, *Science*, 346, 844-7, 2014b.

563

564

565 **Tables**566 **Table 1.** Equivalent dose (D_e), dose rate data and OSL age estimates for Lake Little Llangothlin.

567 Dose rates are listed as attenuated based on published factors (Stokes et al. 2003; Mejdahl 1979).

Sample	D_e (Gy)	K (%)	Th (ppm)	U (ppm)	Beta dose rate (Gy/ka)	Cosmic dose rate (Gy/ka)	Water content (%)	Total dose rate (Gy/ka)	Age (ka)
L-EVA 1228 (LL1)	6.1±0.6	0.53±0.02	4.0±0.2	1.3±0.1	0.6±0.1	0.19±0.02	10±3	1.21±0.07	5.1±0.5
L-EVA 1229 (LL2)	19.2±0.4	0.34±0.02	3.5±0.2	1.3±0.1	0.5±0.1	0.18±0.02	5±3	1.02±0.06	18.9±1.2
L-EVA 1230 (LL3)	26.9±0.9	0.69±0.04	3.0±0.1	1.3±0.1	0.7±0.1	0.18±0.02	7±3	1.30±0.08	20.6±1.4
L-EVA 1231 (LL4)	22.9±1.2	0.56±0.02	2.7±0.1	0.7±0.1	0.5±0.1	0.18±0.02	6±3	0.98±0.05	23.4±1.8

568

569

570 **Figure Legends**

571 **Figure 1.** Geomorphology and sediments at Little Llangothlin Lagoon (30° 5' 9"S, 151° 46' 53"E), 18 km NE Guyra, NSW, showing the locations of GPR transects, sediment cores (right) and the position of OSL samples.

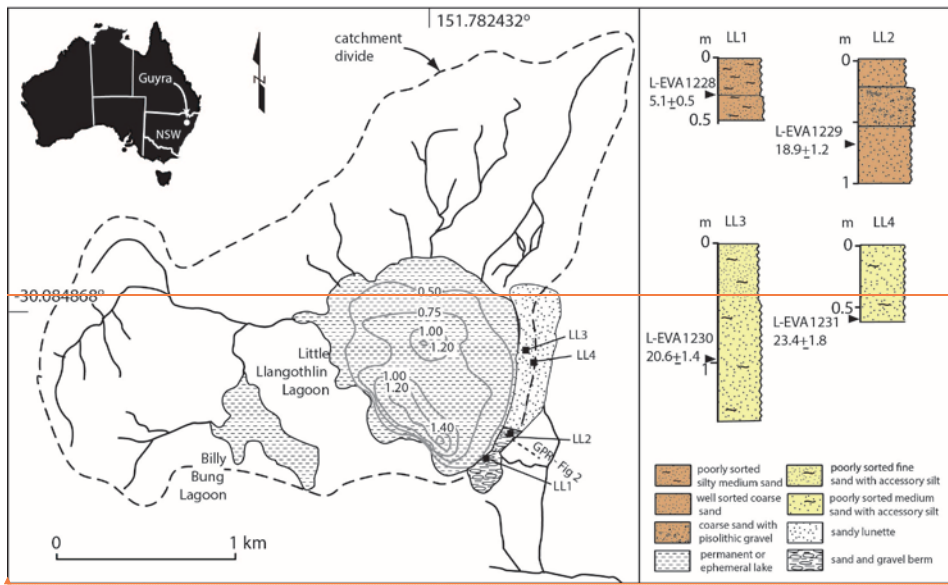
574 **Figure 2a.** GPR transects over the “berm”. See Fig 1. for location of transect. GPR line A7 was acquired perpendicular to the shoreline starting just lakeward of the highest point on the berm. Internal structures are characteristic of an interfingering beach-washover-basin fill sequence over a spit complex. Upper panel, raw data; lower panel, interpretation.

578 **Figure 2b.** GPR line A9 was acquired from the lake shore to the highest point on the berm. Internal structures show characteristics of a beach environment over a spit complex. Top left panel, raw data; top right panel, interpretation. The lower panel shows a conceptual model based on composite GPR profiles suggesting a lower lake facies with spit facies underlying beach, washover and basin fill facies.

583 **Figure 3.** Equivalent dose distributions for the LLL samples, illustrated as radial plots. The shaded populations in each case represent the dominant age peaks; the lines illustrate the other identified populations.

586 **Figure 4.** Rose of 9am wind direction vs wind speed in km/hr at Guyra Hospital, 1332 m AMSL (Bureau of Meteorology, 2014). Only winds above ~22 kph are sand carrying (based on the 12 knot threshold of Fryberger, 1979). Sand drift potential is much stronger in winter (August) than it is in summer (February) because the relationship is a power function of the wind speed and frequency of very strong winds is much lower in summer.

592



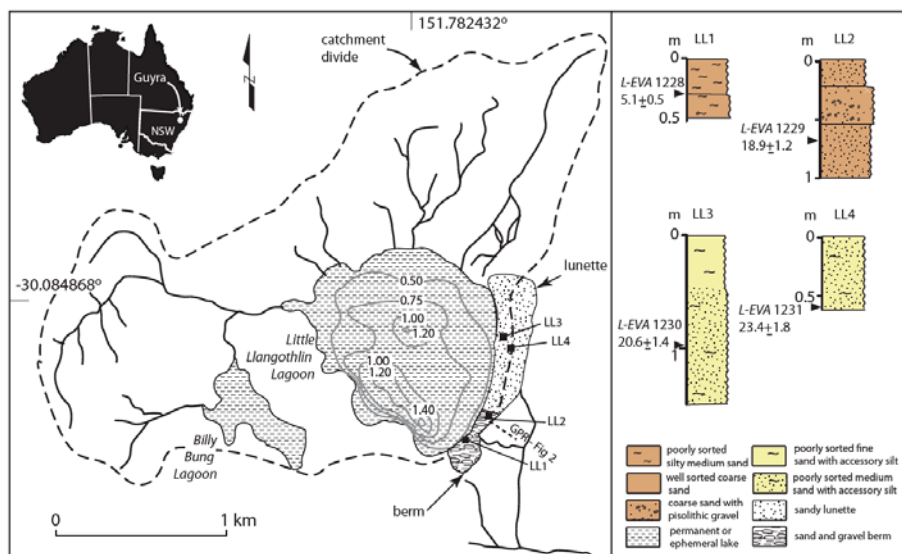
Formatted: Font: Times New Roman

Formatted: Font: Times New Roman

593

594

595



Formatted: Font: Times New Roman

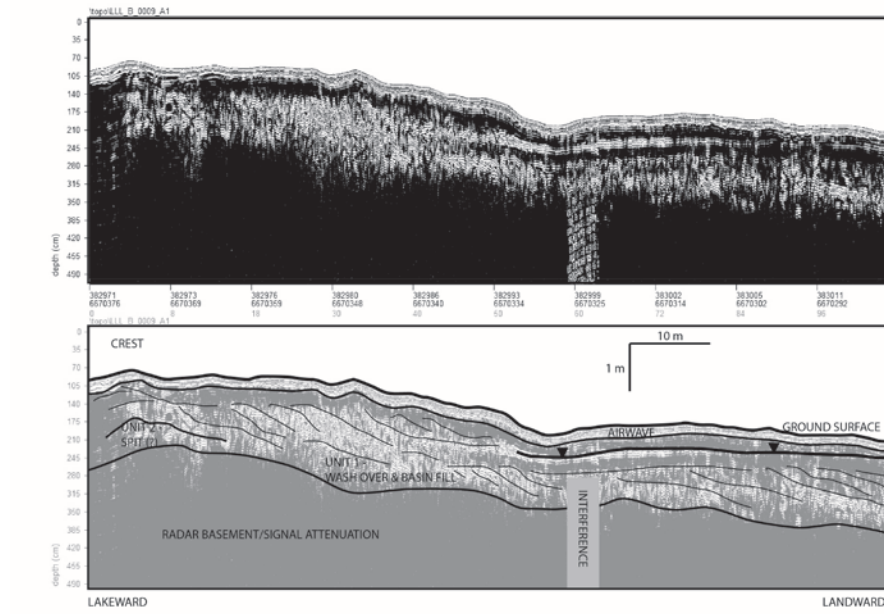
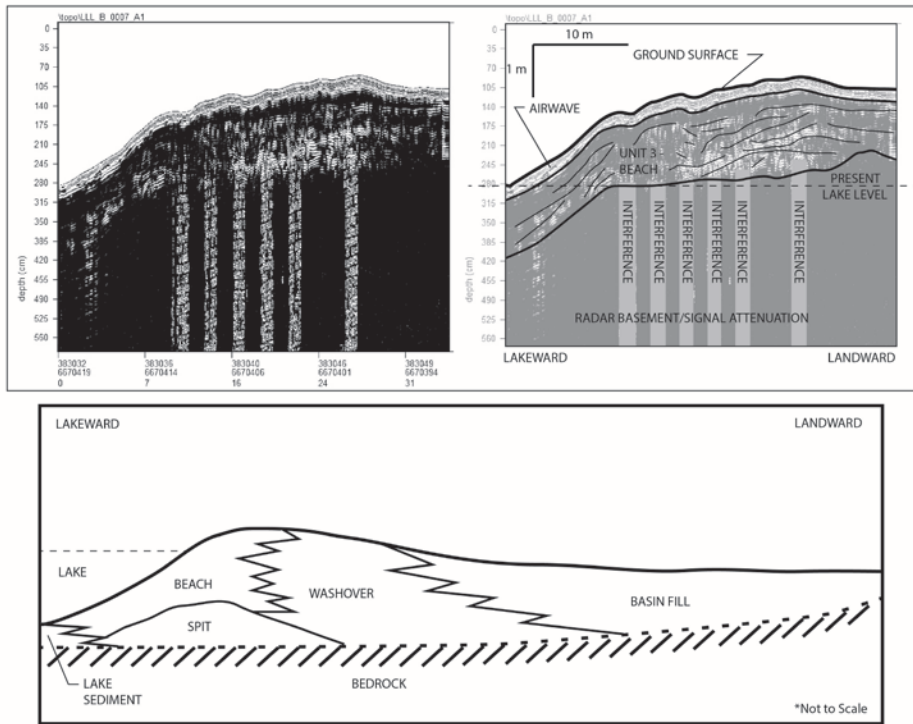


Figure 2a

Formatted: Font: Times New Roman

Formatted: Font: Times New Roman



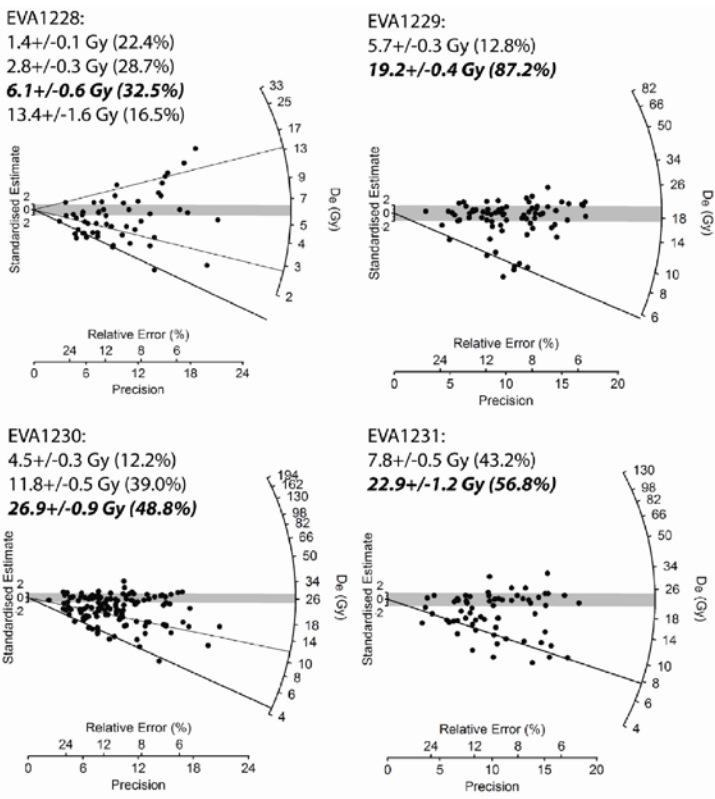
Formatted: Font: Times New Roman

Formatted: Font: Times New Roman

598

599 **Figure 2b**

600



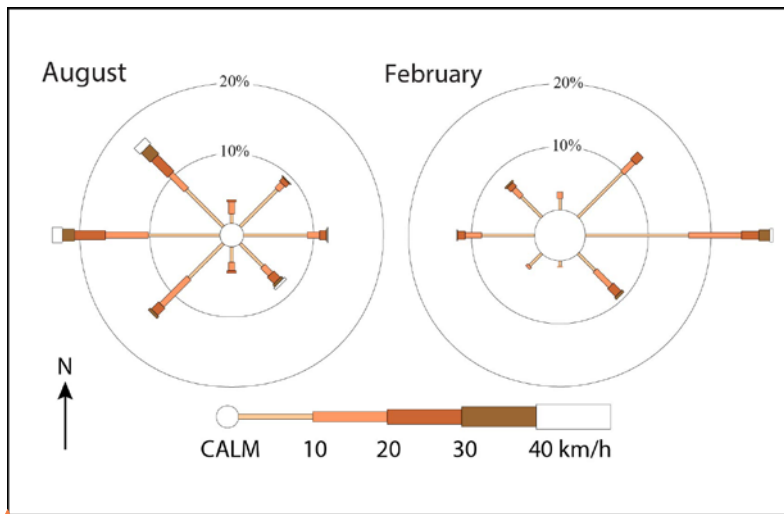
Formatted: Font: Times New Roman

Formatted: Font: Times New Roman

601

602 **Figure 3**

603



604

605 **Figure 4**

606

Formatted: Font: Times New Roman

Formatted: Font: Times New Roman